Available online at www.sciencedirect.com
SCIENCE DIRECT
Inorganica Chimica Acta 359 (2006) 2525–2533
Inorganica Chimica Acta
www.elsevier.com/locate/ica

Dinitrosyl iron complexes $[E_5Fe(NO)_2]^-$ (E = S, Se): A precursor of Roussin's black salt $[Fe_4E_3(NO)_7]^-$

Tai-Nan Chen [a], Feng-Chun Lo [a], Ming-Li Tsai [a], Ko-Nien Shih [b,*], Ming-Hsi Chiang [a], Gene-Hsiang Lee [c], Wen-Feng Liaw [a,*]

[a] Department of Chemistry, National Tsing Hua University, Hsinchu 30043, Taiwan
[b] Department of Radiological Technology, Yuanpei Institute of Science and Technology, Hsinchu, Taiwan
[c] Instrumentation Center, National Taiwan University, Taipei 10764, Taiwan

Received 22 December 2005; received in revised form 17 February 2006; accepted 23 February 2006
Available online 3 March 2006

Abstract

[PPN][$Se_5Fe(NO)_2$] (**1**) and [K-18-crown-6-ether][$S_5Fe(NO)_2$] (**2′**) were synthesized and characterized by IR, UV–Vis, EPR spectroscopy, magnetic susceptibility, and X-ray structure. [PPN][$Se_5Fe(NO)_2$] easily undergoes ligand exchange with S_8 and $(RS)_2$ (R = C_7H_4SN (**5**), *o*-$C_6H_4NHCOCH_3$ (**6**), C_4H_3S (**7**)) to form [PPN][$S_5Fe(NO)_2$] and [PPN][$(SR)_2Fe(NO)_2$]. The reaction displays that $[E_5Fe(NO)_2]^-$ (E = Se (**3**), S (**4**)) facilely converts to $[Fe_4E_3(NO)_7]^-$ by adding acid HBF_4 or oxidant [Cp_2Fe][BF_4] in THF, respectively. Obviously, complexes **1** and **2′** serve as the precursors of the Roussin's black salts **3** and **4**. The electronic structure of $\{Fe(NO)_2\}^9$ core of $[Se_5Fe(NO)_2]^-$ is best described as a dynamic resonance hybrid of $\{Fe^{+1}(\cdot NO)_2\}^9$ and $\{Fe^{-1}(NO^+)_2\}^9$ modulated by the coordinated ligands. The findings, EPR signal of $g = 2.064$ for **1** at 298 K, implicate that the low-molecular-weight DNICs and protein-bound DNICs may not exist with selenocysteine residues of proteins as ligands, since the existence of protein-bound DNICs and low-molecular-weight DNICs in vitro has been characterized with a characteristic EPR signal at $g = 2.03$. In addition, complex **2′** treated human erythroleukemia K562 cancer cells exposed to UV-A light greatly decreased the percentage survival of the cell cultures.

Keywords: Dinitrosyl iron compounds; DNICs; Selenolate

1. Introduction

Extensive EPR studies have identified nitrosyl non-heme iron complexes as products from the interaction of NO with several iron–sulfur and other iron-containing proteins [1–9]. Examples of nitric oxide coordination to iron and the spectroscopic signals of dinitrosyl iron complexes (DNICs) are of much interest, particularly in light of role(s) in sulfur-rich protein uptake and degradation [6,7]. DNICs have been suggested as one of the two possible forms for storage and transport of NO in biological system [8,9]. In vivo, nitric oxide can be stabilized and stored in the form of dinitrosyl iron complexes with proteins (protein-bound DNICs) and is probably released from cells in the form of low-molecular-weight dinitrosyl iron complexes (LMW-DNICs) [6–10]. Recent report showed that both cysteine-bound DNICs (DNICs-CYS) and glutathione-bound DNICs (DNICs-GSH) elicited a NO release associated relaxant effect in isolated arteries, and a faster rate of NO release from DNICs-CYS than from DNICs-GSH was observed [11]. The chemical versatility of sulfur in biology is well established [12]. A genetic cordon for selenocysteine incorporation into proteins has been established in prokaryotes in the past decade [13]. In fact, Böck et al. pronounced selenocysteine as the 21st amino acid in ribosome-mediated protein synthesis [14].

In particular, nitric oxide derived from spontaneously decomposing NO-donor compounds, e.g., Roussin's salt, has been known to sensitize hypoxic cell cultures to

* Corresponding authors. Tel./fax: +88635721890.
E-mail address: wfliaw@mx.nthu.edu.tw (W.-F. Liaw).

0020-1693/$ - see front matter © 2006 Elsevier B.V. All rights reserved.
doi:10.1016/j.ica.2006.02.035

γ-radiation damage [15]. In model compounds, Glidewell and co-workers reported that reactions of iron–sulfur proteins model compounds $[Fe_2(\mu\text{-}S)_2\ (S,S\text{-}C_6H_4)_2]^{2-}$/$[Fe_4S_4(SR)_4]^{2-}$ and nitric oxide/nitrite, followed by acidic work-up, yielded the anionic $[Fe_4S_3(NO)_7]^-$ via the formation of the paramagnetic intermediate $[(SH)_2Fe(NO)_2]^-$ [16,17]. Also, Roussin's black salt $[Fe_4S_3(NO)_7]^-$ was reported to be isolated upon reaction of $[Fe(CO)_3(NO)]^-$ with elemental sulfur or polysulfide [18], and protonation of $[Fe_2S_2(NO)_4]^{2-}$ by HBF_4/CF_3COOH [19]. Interestingly, the facile conversion of $[Fe_2S_2(NO)_4]^-$ into $[Fe_4S_3(NO)_7]^-$ was also observed simply by dissolving $[Fe_2S_2(NO)_4]^-$ salt in CH_2Cl_2 [16,20].

We have demonstrated that reversible transformation of the $\{Fe(NO)_2\}^9$ [PPN][$S_5Fe(NO)_2$] (PPN = bis(triphenylphosphoranylidene)ammonium) to the $[S_5Fe(\mu\text{-}S)_2FeS_5]^{2-}$ cluster by photolysis in the presence of the NO-acceptor reagent $[(C_4H_8O)Fe(S,S\text{-}C_6H_4)_2]^-$, identified by UV–Vis, EPR and IR [21,22], is consistent with reports of repair of nitric oxide modified [2Fe–2S] ferredoxin by cysteine desulfurase and L-cysteine in vitro [23]. A logical and significant extension of these efforts would be analogous studies involving exploration of dinitrosyl iron derivatives in the biologically relevant selenolate ligand field. In this study, the analogue [PPN][$Se_5Fe(NO)_2$] (**1**) was isolated from reaction of [PPN][$Fe(CO)_3(NO)$] and Se powder in THF. The facile conversion of complexes **1**/[cation][$S_5Fe(NO)_2$] (cation = $N(PPh_3)_2$ (**2**), K-18-crown-6-ether (**2′**)) into Roussin's black salts $[Fe_4E_3(NO)_7]^-$ (E = Se (**3**), S (**4**)) accompanied by the release of NO was observed upon reaction of complexes **1/2** and $HBF_4/[Cp_2Fe][BF_4]$, individually. Transformation of complex **1** to dinitrosyl iron complexes [PPN][$(RS)_2Fe(NO)_2$] (R = C_7H_4SN (**5**), *o*-$C_6H_4NHCOCH_3$ (**6**), C_4H_3S (**7**)) was also investigated. In this paper, we also demonstrate that NO is able to transfer from $[S_5Fe(NO)_2]^-$ to the NO-trapping reagents ($[Fe^{II}(S_2CN(Et)_2)_2]$ or $[Fe^{III}(S_2CN(Et)_2)_3]$) to form $[(NO)Fe(S_2CN(Et)_2)_2]$ complex. Also described are effects on the mortalities of human erythroleukemia K562 cells treated with DNICs **2′** alone and DNICs **2′** combined with UV-A light (wavelength = 400–315 nm).

2. Experimental

Manipulations, reactions, and transfers of samples were conducted under nitrogen according to standard Schlenk techniques or in a glovebox (argon gas). Solvents were distilled under nitrogen from appropriate drying agents (diethyl ether from CaH_2, acetonitrile from P_2O_5–CaH_2, methylene chloride from P_2O_5–CaH_2, hexane and tetrahydrofuran (THF) from sodium-benzophenone) and stored in dried, N_2-filled flasks over 4 Å molecular sieves. Nitrogen was purged through these solvents before use. Solvent was transferred to a reaction vessel via a stainless steel cannula under positive pressure of N_2. The reagents bis(triphenylphosphoranylidene)ammonium chloride ([PPN]Cl), iron pentacarbonyl, sodium nitrite, elemental sulfur, selenium powder, fluoroboric acid, ferrocenium tetrafluoroborate, (Lancaster/Aldrich/Fluka/Acros), and 3-(4,5-dimethylthiazol-2-yl)-5-diphenyltetrazolium bromide (MTT) (Sigma) were used as received. The compounds [PPN][$Fe(CO)_3(NO)$], $[Fe^{II}(S_2CN(Et)_2)_2]$ ($Fe(DTC)_2$), and $[Fe^{III}(S_2CN(Et)_2)_3]$ ($Fe(DTC)_3$), were synthesized and characterized by published procedures [24,28]. Infrared spectra of the ν_{NO} stretching frequencies were recorded on a Perkin–Elmer model spectrum one spectrophotometer with sealed solution cells (0.1 mm) and KBr windows. UV–Vis spectra were recorded on a GBC Cintra 10e spectrophotometer. Analyses of carbon, hydrogen, and nitrogen were obtained with a CHN analyzer (Heraeus).

2.1. Preparation of [PPN][$Se_5Fe(NO)_2$] (1)

The compounds [PPN][$Fe(CO)_3(NO)$] (0.708 g, 1 mmol) and Se powder (0.48 g, 6 mmol) were dissolved in 10 mL of THF and refluxed under nitrogen at 70 °C. The reaction was monitored with FTIR. The spectrum (IR (THF): 1736 s, 1697 s (ν_{NO}) cm^{-1}) was assigned to the formation of complex **1**. The resulting mixture was filtered to separate dark green solution (complex **1**) and dark brown insoluble solid. The dark green THF solution was then concentrated and diethyl ether–hexane was added to precipitate the dark green solid [PPN][$Se_5Fe(NO)_2$] (**1**) (0.423 g, yield 40%, based upon total iron). Diffusion of diethyl ether into THF solution of complex **1** at −15 °C for 4 weeks led to dark green crystals suitable for X-ray crystallography. IR (THF): 1736 s, 1697 s (ν_{NO}) cm^{-1}. Absorption spectrum (THF) [λ_{max}/nm ($\varepsilon/M^{-1}\,cm^{-1}$)]: 444 (3168), 588 (1378) (Calc. for $C_{36}H_{30}N_3O_2P_2Se_5Fe$: C, 53.07; H, 3.71; N, 5.16. Found: C, 53.29; H, 3.90; N, 5.58%).

2.1.1. Preparation of [K-18-crown-6-ether][$S_5Fe(NO)_2$] (2′)

[K-18-crown-6-ether][$Fe(CO)_3NO$] (0.484 g, 1 mmol) and S_8 (0.256 g, 1 mmol) were loaded into a 50-mL Schlenk flask and dissolved in THF (10 mL). After the solution mixture was stirred under nitrogen at ambient temperature overnight, the solution IR spectrum (IR (THF): 1696 s, 1738 s (ν_{NO}) cm^{-1}) was assigned to the formation of [K-18-crown-6-ether][$S_5Fe(NO)_2$]. The resulting mixture was then filtered through Celite and diethyl ether was then added to precipitate dark-brown solid [K-18-crown-6-ether][$S_5Fe(NO)_2$] (**2′**) (yield 0.20 g, 35%) [21]. Diffusion of diethyl ether into THF solution of complex **2′** at −15 °C for 4 weeks led to dark-brown crystals suitable for single-crystal X-ray diffraction. IR (THF): 1738 s, 1696 s (ν_{NO}) cm^{-1}. Absorption spectrum (THF) [λ_{max}/nm ($\varepsilon/M^{-1}\,cm^{-1}$)]: 364 (2887), 440 (2824), 568 (916).

2.2. Reactions of [PPN][$E_5Fe(NO)_2$] (E = Se (1); S (2)) and [Cp_2Fe][BF_4]/HBF_4

A THF solution (2 mL) of [Cp_2Fe][BF_4] (0.0273 g, 0.1 mmol) (or fluoroboric acid (17.8 μL, 0.1 mmol)) was

added dropwise by a cannula into the THF solution (3 mL) of complex **1** (0.1045 g, 0.1 mmol) (or complex **2** (0.1 mmol)) and stirred at room temperature overnight. The reaction mixture was filtered to remove the insoluble solid and then hexane was added to precipitate the known dark green solid [PPN][$Fe_4E_3(NO)_7$] (E = S (**3**), Se (**4**); yield 65% for **3** and 21% for **4**) [25–27]. Complex **3**: IR (THF): 1795 w, 1743 s, 1707 w (ν_{NO}) cm^{-1}. Complex **4**: IR (THF):1790 w, 1740 s, 1707 w (ν_{NO}) cm^{-1}. Recrystallization from saturated THF solution of complexes **3/4** with hexane diffusion at −15 °C gave dark green crystals suitable for X-ray crystallography.

2.3. Reaction of [PPN][$Se_5Fe(NO)_2$] and disulfides $(RS)_2$ (R = 2-C_7H_4NS, C_4H_3S, C_6H_4-o-NHC(O)CH_3)

A THF solution of [PPN][$Se_5Fe(NO)_2$] (0.209 g, 0.2 mmol) was transferred into a 50-mL Schlenk flask loaded with disulfide species $(RS)_2$ (R = 2-C_7H_4NS (0.067 g, 0.2 mmol), C_4H_3S (0.046 g, 0.2 mmol), C_6H_4-*o*-NHC(O)CH_3 (0.067 g, 0.2 mmol)). The reaction mixture was stirred for 10 min at room temperature, then filtered to remove the insoluble solid, and hexane (15 mL) was added to precipitate the known [PPN][$(RS)_2Fe(NO)_2$] (R = C_7H_4NS (**5**) (79%), C_6H_4-*o*-NHC(O)CH_3 (**6**) (80%), C_4H_3S (**7**) (88%)), characterized by IR, UV–Vis, and single-crystal X-ray diffraction [22]. Complex **5**: IR (THF): 1766 s, 1716 s (ν_{NO}) cm^{-1}. Absorption spectrum (THF) [λ_{max}/nm (ε/M^{-1} cm^{-1})]: 465 (3500), 799 (712). Complex **6**: IR (THF): 1752 s, 1705 s (ν_{NO}), 1690 s (ν_{CO}) cm^{-1}. Absorption spectrum (THF) [λ_{max}/nm (ε/M^{-1} cm^{-1})]: 479 (2984), 774 (453). Complex **7**: IR (THF): 1743 s, 1698 s (ν_{NO}) cm^{-1}. Absorption spectrum (THF) [λ_{max}/nm (ε/M^{-1} cm^{-1})]: 514 (2830), 798 (902) [22].

2.4. Photolysis of THF solution of complex **1** and [PPN]$_2$[Fe(S,S-C_6H_4)$_2$]$_2$

An 8 mL THF solution of compounds **1** (0.0525 g, 0.05 mmol) and $[PPN]_2[Fe(S,S\text{-}C_6H_4)_2]_2$ (0.089 g, 0.05 mmol) was loaded into a reactor (20 mL). The reaction mixture was then irradiated by UV lamp (I_{max} = 366 nm) under N_2 atmosphere at room temperature for 6 h after the reaction solution was stirred in the dark for 2 h. The resulting mixture was filtered to separate the red brown precipitate and the dark reddish brown upper solution. The uncharacterized dark brown precipitate is insoluble in organic solvent. IR (ν_{NO} 1789 cm^{-1}) and UV–Vis spectra (497, 610, 1305 nm (THF)) of the filtrate (upper solution) indicated the formation of $[PPN][(NO)Fe(S,S\text{-}C_6H_4)_2]$. The THF solution of complex $[PPN][(NO)Fe(S,S\text{-}C_6H_4)_2]$ was concentrated to 5 mL under vacuum and hexane–diethyl ether was then added to precipitate the dark reddish brown solid $[PPN][(NO)Fe(S,S\text{-}C_6H_4)_2]$ (0.080 g, 40%) identified by UV–Vis (497, 610, 1305 nm (THF)), and FTIR (ν_{NO}: 1789 s cm^{-1} (THF)).

2.5. Reaction of [PPN][$S_5Fe(NO)_2$], $Fe(DTC)_3$ (DTC = diethyldithiocarbamate) and S_8

A solution containing [PPN][$S_5Fe(NO)_2$] (0.1 mmol, 0.0815 g) and S_8 (0.1 mmol, 0.0256 g) and $Fe(DTC)_3$ (0.1 mmol, 0.05 g) (or $Fe(DTC)_2$ (0.2 mmol, 0.0704 g)) [28] in THF (10 mL) was stirred overnight under N_2 (g) at ambient temperature. The reaction solution was monitored by IR. The spectrum (IR (THF): 1715 s (ν_{NO}) cm^{-1}) was assigned to the formation of the known $[(NO)Fe(DTC)_2]$ [28]. The reaction mixture was then filtered to separate the green solution $[(NO)Fe(DTC)_2]$ and the known reddish-brown precipitate [PPN][$S_5Fe(\mu\text{-}S)_2FeS_5$] (yield 62%, based on total iron) characterized by UV–Vis and single-crystal X-ray diffraction [29,30].

2.6. Cell culture experiment

Human erythroleukemia K562 cells were grown in suspension in Dulbecco's modified Eagle's medium (DMEM) supplemented with 10% fetal bovine serum (Hyclone), penicillin (100 IU/ml), streptomycin (100 μg/ml), Fungizone (50 μg/ml) and 2 mM L-glutamine. The cells were maintained at 37 °C under 5% CO_2 in a humidified incubator. The cells were plated in 12-well plates at cell density of 2×10^5, 3×10^5, and 4×10^5 cells/well, respectively. Complex [18-crown-6-ether-K][$S_5Fe(NO)_2$] (**2′**) serves as a NO-donor reagent. The cells were treated with different concentrations of **2′** (1, 10, and 100 μM) for 24 h and the percentage of survival was measured by the colorimetric MTT assay. The MTT solution (5 mg/ml in PBS) was added to each well and then incubated for 3 h. The surviving cells convert MTT to MTT formazan that shows purple color when formazan was dissolved in dimethyl sulfoxide (DMSO), and the absorption intensity was measured at 570 nm by using a microplate reader for enzyme-linked immunosorbent assays (ELx808). Complex **2′** proved to be not cytotoxic or cytostatic to be used in such experiments. The cells were treated with compound **2′** (10 μM) for 2 h in DMEM and then exposed the cell to UVA light (λ = 430 nm) for 10 min. The cells were then cultured for 24 h after DNIC and UVA treatment. The collected cells were centrifuged in 1000 rpm for 1 min to separate the medium. Fresh DMEM was added and subsequently the viability was determined by the colorimetric MTT assay.

2.7. EPR measurements

EPR measurements were performed at X-band using a Bruker EMX spectrometer equipped with a Bruker TE102 cavity and a Bruker VT2000 temperature control unit (120–300 K). For liquid helium temperature measurements, an Oxford ESR910 continuous flow cryostat (4–200 K) was used. X-band EPR spectra of complex **1** frozen in THF were obtained with a microwave power of 5 mW, frequency at 9.4323 GHz, and modulation amplitude of 0.05 mT at 100 kHz (temperature = 77 K). X-band EPR

spectra of complex **1** were measured at a frequency of 9.78410 GHz at room temperature.

2.8. Magnetic measurements

The magnetization data were recorded on a SQUID magnetometer (MPMS5 Quantum Design company) with an external 0.5 T magnetic field for complex **1** in the temperature range from 4 to 300 K. The experimental magnetic susceptibility data were corrected for diamagnetism by the tabulated Pascal's constants.

2.9. Crystallography

Crystallographic data of complexes **1** and **2′** are summarized in the Supporting Information. The crystals of **1** and **2′** chosen for X-ray diffraction studies measured $0.25 \times 0.20 \times 0.20$ mm and $0.30 \times 0.25 \times 0.25$ mm, respectively. Each crystal was mounted on a glass fiber. Diffraction measurements for complexes **1** and **2′** were carried out at 150(1) K on a Bruker-Nonius Kappa CCD diffractometer with graphite-monochromated Mo Kα radiation ($\lambda =$ 0.7107 Å) and θ between 1.45° and 27.50° for complex **1**, and between 1.43° and 27.50° for complex **2′**. Least-squares refinement of the positional and anisotropic thermal parameters for the contribution of all non-hydrogen atoms and fixed hydrogen atoms was based on F^2. Absorption correction was made using SORTAV [31]. The SHELXTL structure refinement program was employed [32]. In the case of complexes **1** and **2′**, the $[Se_5Fe(NO)_2]$ and $[S_5Fe(NO)_2]$ fragments were found at disordered positions ($[S_5Fe(NO)_2]:[Se'_5Fe'(N'O')_2] = 0.94:0.06$ and $[S_5Fe(NO)_2]:[S'_5Fe'(N'O')_2] = 0.5:0.5$), respectively, and were refined by partial occupancies.

3. Results and discussion

3.1. Synthesis and spectroscopic characterization

As presented in Scheme 1a, a straightforward synthetic reaction of [PPN][$Fe(CO)_3(NO)$] with six equivalents of Se powder in THF at 70 °C was conducted. The reaction mixture led to the isolation of the THF-soluble dark brown [PPN][$Se_5Fe(NO)_2$] (**1**) (Fig. 1). Complex **1** exhibits two IR ν_{NO} bands at 1736 s, 1697 s cm^{-1} (THF). The ν_{NO} bands of complex **1** are similar to the NO stretching frequencies of $[S_5Fe(NO)_2]^-$ ($\nu_{NO} = 1739$, 1695 cm^{-1}), $[(PhS)_2Fe(NO)_2]^-$ ($\nu_{NO} = 1735$, 1694 cm^{-1}) [21,22], and $[(PhSe)_2Fe(NO)_2]^-$ (1741 s, 1697 s cm^{-1} (CH_2Cl_2)) [33]. Thus, the electron-donating ability of the $[Se_5]^{2-}$ ligand to $\{Fe(NO)_2\}$ unit could be considered as the same as those of the $[S_5]^{2-}$, 2[$SePh]^-$ and 2[$SPh]^-$ ligands, respectively [21,22,33,34], where the iron–dinitrosyl unit has the formal electronic assignment, $\{Fe(NO)_2\}^9$ [35]. In contrast to the EPR isotropic signal at $g = 2.03$, the characteristic of dinitrosyl iron complexes $[(RS)_2Fe(NO)_2]^-$, complex **1** exhibits an isotropic signal at $g = 2.064$ at 298 K (Fig. 2a), and a

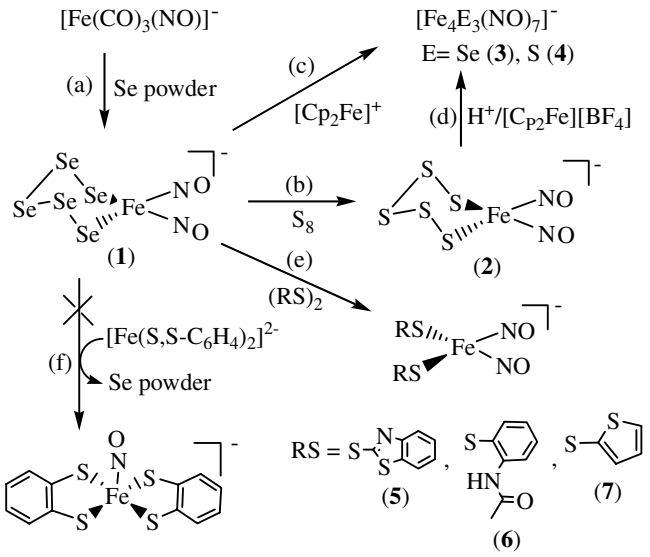

Scheme 1.

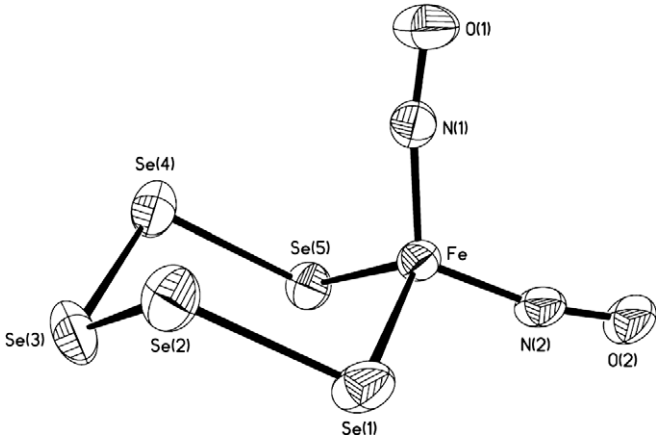

Fig. 1. ORTEP drawing and labeling scheme of the $[(NO)_2FeSe_5]^-$ anion with thermal ellipsoids drawn at 50% probability.

$S = 1/2$ rhombic EPR spectrum with principal g values at $g_1 = 2.016$, $g_2 = 2.034$, and $g_3 = 2.146$ (77 K) (Fig. 2b) [6,9,21–23]. Replacing the sulfur ring with selenium ring yielded the obvious changes of the EPR spectra indicating that the unpaired electron is more localized in the $\{Fe(NO)_2\}^9$ unit [21,22].

3.2. Reactivity

The coordinated $[Se_5]^{2-}$ ligand of complex **1** could be replaced by the $[S_5]^{2-}$. Dark green solution of complex **1** with one equivalent of S_8 in THF solution rapidly resulted in color change to dark brown with little NO stretching frequency shift from 1697, 1736 to 1695, 1739 cm^{-1} for $[PPN]^+$ salt and 1696, 1738 cm^{-1} for [K-18-crown-6-ether]$^+$ salt, which implicated the formation of [cation][$S_5Fe(NO)_2$] (cation = PPN (**2**), K-18-crown-6-ether (**2′**)) (Scheme 1b) [21,22]. This substitution reaction is

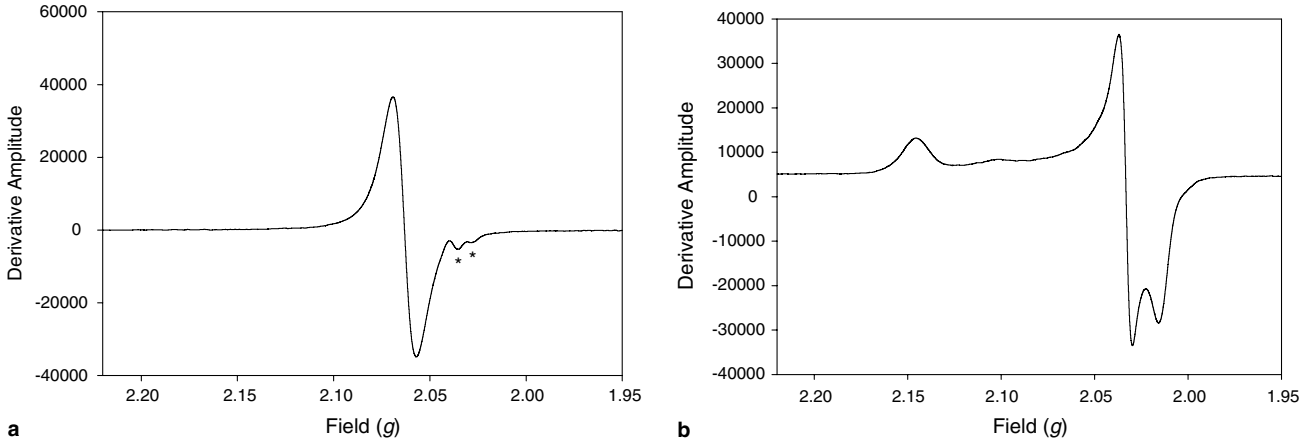

Fig. 2. X-band EPR spectra of complex **1** (a) at 298 K (* indicates impurity), and (b) at 77 K.

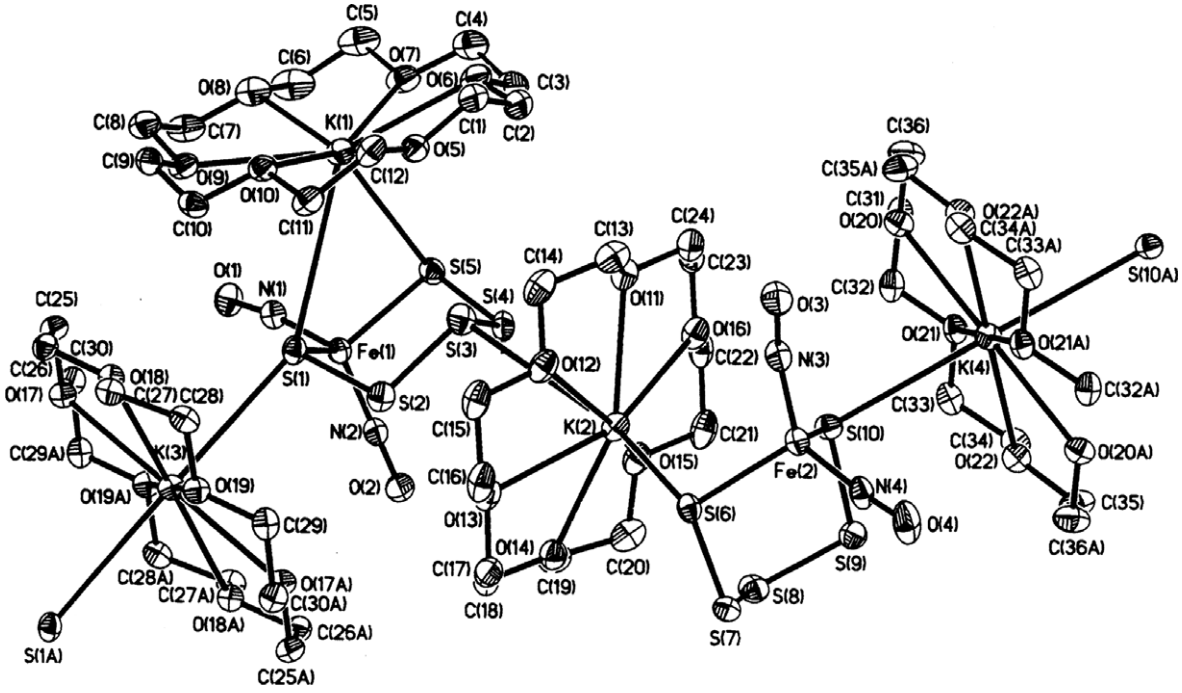

Fig. 3. ORTEP drawing and labeling scheme of [K-18-crown-6-ether][$(NO)_2FeS_5$] with thermal ellipsoids drawn at 30% probability.

expected to be driven by the formation of six-membered-ring FeS_5 bonds that are sufficient to place the $\{Fe(NO)_2\}^9$ complex **2** in the more optimum electronic condition [22]. In contrast, complex **2** was stable in the presence of six equivalents of Se in THF at 70 °C. Also, a difference in the photochemical behavior was observed between the highly photosensitive (photoreactive) complex **2** and photostable complex **1** in the absence of NO-trapping agent $[Fe(S,S\text{-}C_6H_4)_2]_2^{2-}$.

As shown in Scheme 1c–d, complexes **1** and **2** reacted with one equivalent of acid HBF_4 (or oxidant $[Cp_2Fe][BF_4]$) in THF at ambient temperature overnight yielded the known dark green complexes $[Fe_4E_3(NO)_7]^-$ (E = Se (**3**), S (**4**)), respectively [9,15–17], as identified by IR ν_{NO} (1790 w, 1740 s, 1707 w (THF) (**3**); 1795 w, 1743 s, 1707 w cm^{-1} (THF) (**4**)). The products are further confirmed by X-ray diffraction analysis. Obviously, the mononuclear dinitrosyl iron complexes **1** and **2** are the precursors of complexes **3** and **4** in this reaction, providing a route for reassembly in reactions involving a change of nuclearity and release of NO.

In contrast to the inertness of reaction of complex **2** and disulfides $(RS)_2$ [22], complex **1** triggers the S–S bond activation of $(RS)_2$ species to form the stable $[(RS)_2Fe(NO)_2]^-$ (R = C_7H_4SN (**5**), *o*-$C_6H_4NHCOCH_3$ (**6**), C_4H_3S (**7**)) as indicated in the NO stretching frequency shift from 1736, 1697 to 1766, 1716, 1752, 1705, and 1743, 1698 cm^{-1}, respectively (Scheme 1e) [22]. This result may implicate that the $\{Fe(NO)_2\}^9$ core shows more affinity to the thiolate ligands as compared to selenolate ligand.

In our previous report [21,22], we have demonstrated the reversible transformation between $[S_5Fe(NO)_2]^-$ and $[S_5Fe(\mu\text{-}S)_2FeS_5]^{2-}$. Reactions of $[S_5Fe(NO)_2]^-$ and NO trapping agent $[Fe(S,S\text{-}C_6H_4)_2]_2^{2-}$ in DMSO yielded $[(NO)Fe(S,S\text{-}C_6H_4)_2]^-$ and $[S_5Fe(\mu\text{-}S)_2FeS_5]^{2-}$ with $k_{obs} = 1.5\ (3) \times 10^{-2}\ s^{-1}$ (DMSO, 18 °C). For comparisons of NO-release activity of dinitrosyl iron–thiolate and iron–selenolate compounds, the representative time courses (6 h) of NO release trapped by one equivalent of $[Fe(S,S\text{-}C_6H_4)_2]_2^{2-}$ in THF were monitored by the formation of $[(NO)Fe(S,S\text{-}C_6H_4)_2]^-$ with an intense absorption band at 1298 nm. The stability of complexes **1**/$[(PhSe)_2Fe(NO)_2]^-$ displaying a nearly identical UV–Vis absorption spectrum suggests that the NO release of complexes **1**/$[(PhSe)_2Fe(NO)_2]^-$ does not occur directly in the presence of NO-trapping agent $[Fe(S,S\text{-}C_6H_4)_2]_2^{2-}$ at ambient temperature (Scheme 1f). This result demonstrates that $\{Fe(NO)_2\}^9$ $[Se_5Fe(NO)_2]^-$ and $[(PhSe)_2Fe(NO)_2]^-$ display the poor NO-donor activity. Obviously, the selenium or sulfur bound to the $\{Fe(NO)_2\}^9$ motif may serve to modulate the NO-release ability of DNICs. Such a regulatory role of thiolate/selenolate ligands of the $\{Fe(NO)_2\}^9$ DNICs may be critical for $\{Fe(NO)_2\}^9$ DNICs to serve as a NO transporter in biological systems. However, irradiation of THF solution of complex **1** in the presence of NO-trapping agent $[Fe(S,S\text{-}C_6H_4)_2]_2^{2-}$ for 6 h partially yielded $[(NO)Fe(S,S\text{-}C_6H_4)_2]^-$ (yield 40%) and Se powder. Presumably, irradiation triggers NO release of complex **1**. Photolysis of THF solution of $[(PhSe)_2Fe(NO)_2]^-$ for 1 h yielded insoluble solids (complete decomposition). The facile release of NO under photolysis for Roussin's red/black salts has been studied by Ford et al [15].

Interestingly, reaction of complex **1** with one equivalent of $[Fe(S,S\text{-}C_6H_4)_2]_2^{2-}$ in the presence of additional S_8 powder under photolysis resulted in the formation of $[(NO)Fe(S,S\text{-}C_6H_4)_2]^-$, Se powder and the dianionic $[S_5Fe(\mu\text{-}S)_2FeS_5]^{2-}$ isolated in ~70% yield [29,30]. Formation of the mixed-chalcogenide $[Se_5Fe(\mu\text{-}S)_2FeSe_5]^{2-}$ and $[Se_5Fe(\mu\text{-}Se)_2FeSe_5]^{2-}$ from reaction of complex **1**, S_8 powder and $[Fe(S,S\text{-}C_6H_4)_2]_2^{2-}$ under photolysis was not observed. Obviously, ligand-exchange reaction preceded NO release forming $[S_5Fe(NO)_2]^-$, and subsequent NO release accompanied by oxidative addition to yield $[S_5Fe(\mu\text{-}S)_2FeS_5]^{2-}$ via intermediate $[S_5Fe^{I}]$ [21].

In order to further demonstrate that complex **2** primarily transports NO radical, the following reactions were conducted. Reaction of complex **2** and two equivalents of $[Fe(S,S\text{-}CN(Et)_2)_2]$ in the presence of one equivalent of S_8 in THF at ambient temperature afforded the known $[(NO)Fe(S,S\text{-}CN(Et)_2)_2]$ and $[S_5Fe(\mu\text{-}S)_2FeS_5]^{2-}$ immediately, as characterized by IR, UV–Vis and X-ray diffraction [28–30]. Whereas only one equivalent of $[Fe(S,S\text{-}CN(Et)_2)_3]$ was required to completely convert pne equivalent of complex **2** into $[S_5Fe(\mu\text{-}S)_2FeS_5]^{2-}$ along with the formation of $[(NO)Fe(S,S\text{-}CN(Et)_2)_2]$ in the presence of one equivalent of S_8, consistent with the trapping specificity of different redox forms, $[Fe^{II}(S,S\text{-}CN(Et)_2)_2]$ versus $[Fe^{III}(S,S\text{-}CN(Et)_2)_3]$ for NO radical [28]. In a similar fashion, reaction of complex **1** and one equivalent of $[Fe(S,S\text{-}CN(Et)_2)_3]$ led to the isolation of $[(NO)Fe(S,S\text{-}CN(Et)_2)_2]$ and Se powder (no repaired product $[Se_5Fe(\mu\text{-}Se)_2FeSe_5]^{2-}$ was isolated) in THF overnight. Compared to complex **2**, the prolonged reaction time for the complete formation of $[(NO)Fe(S,S\text{-}CN(Et)_2)_2]$ from reaction of complex **1** and one equivalent of $[Fe(S,S\text{-}CN(Et)_2)_3]$ also implicates the less NO-release ability of complex **1**.

3.3. Magnetic susceptibility study

Magnetic susceptibility data of a powdered sample of complex **1** were collected in the temperature range of 4.00–300 K in a 5 kG (0.5 T) applied field. The net molar magnetic susceptibility (χ_M), as shown in Fig. 4, increases from $4.516 \times 10^{-3}\ cm^3\ mol^{-1}$ at 300 K to $0.097\ cm^3\ mol^{-1}$ at 4 K. Its corresponding $\chi_M T$ value and effective magnetic moment (μ_{eff}) decrease from $1.355\ cm^3\ K\ mol^{-1}$ (3.293 BM) at 300 K to $0.390\ cm^3\ K\ mol^{-1}$ (1.767 BM) at 4 K. From a magnetochemical point of view, the $\{Fe^{+1}(NO)_2\}^9$ unit is considered as a tri-spin system. The spin-only ($g = 2.00$) $\chi_M T$ and μ_{eff} values for three magnetically independent centers are $2.625\ cm^3\ K\ mol^{-1}$ and 4.583 BM, respectively. The spin-only values for the $S = 5/2$ and

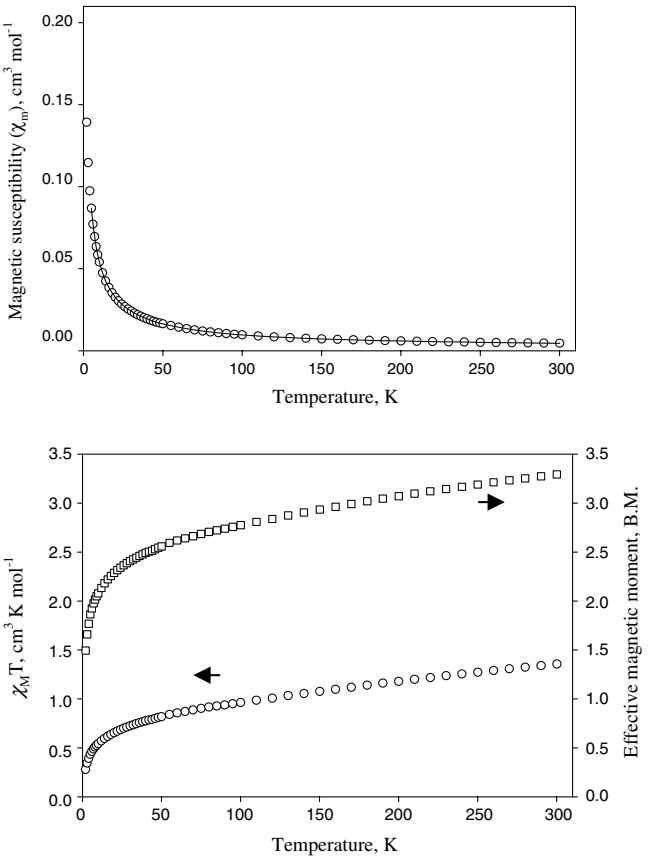

Fig. 4. Plots of molar magnetic susceptibility (top) and effective magnetic moment as well as $\chi_M T$ (bottom) vs. temperature for complex **1**. The solid line is the best fit of the data to the appropriate theoretical expression.

$S = 1/2$ systems are 4.375 cm^3 K mol^{-1} (5.916 BM) and 0.375 cm^3 K mol^{-1} (1.732 BM), respectively.

The theoretical equations for data-fitting are derived from the Heisenberg Hamiltonian ($\hat{H} = -2J\hat{S}_1\hat{S}_2$) and the Van-Vleck equation for a single-J-value system in which J is the exchange parameter between the Fe^+ ion and the $^{\bullet}NO$ radical under approximation of an ideal C_{2v} symmetry. Representation of the electronic state based on the Enemark–Feltham model as $\{Fe(NO)_2\}^9$ for complex **1** is due to the variable nature of NO coordinated to transition metal as M^{n-1}–NO^+, M^n–$NO^{\bullet}$ and M^{n+1}–NO^-. If only the lowest-energy electronic state is considered, both of $\{Fe^+(^{\bullet}NO)_2\}^9$ and $\{Fe^{-1}(^+NO)_2\}^9$ in complex **1** are possible. Both states are paramagnetic. The former has its S_T either of 5/2 or of 1/2. The latter consists of a spin-only value of 1/2. The experimental magnetic susceptibility may be contributed from both electronic states if mixed electronic states are present in complex **1** (equation is shown below). Due to the undetermined exclusive electronic state of complex **1**, fitting of the magnetic data is based on assumption of the presence of both electronic states

$$\chi_M^{exp} = (1-p)\chi_M(\{Fe^+(^{\bullet}NO)_2\}^9) + p\chi_M(\{Fe^-(^+NO)_2\}^9).$$

A least-squares fit ($R^2 = 0.997$) to the χ_M versus temperature (4–180 K) curve, shown as a solid line in Fig. 4, gave $2J = -9\,(1)$ cm^{-1}, $g = 2.14$, $p = 0.812\,(6)$, with TIP (temperature-independent-paramagnetism) held constant at 200×10^{-6} cm^3 mol^{-1}. The result from the fit indicates that dominant fraction of $\{Fe^{-1}(^+NO)_2\}^9$ exists in the electronic structure of complex **1**. In other words, $[(NO)_2FeSe_5]^-$ cannot be a good reagent for the purpose of NO delivery. The retarded NO-release ability of complex **1** was experimentally revealed to compliment the magnetic fitting result. In the presence of $[Fe(S,S\text{-}C_6H_4)_2]_2^{2-}$, all derivatives of DNICs $[(NO)_2Fe(SR)_2]^-$ showed rapid reactions of NO removal [22]. However, most of complex **1** remained in the solution under the same condition after 18 hours. Longer reaction duration did not improve the yield of $[(NO)Fe(S,S\text{–}C_6H_4)_2]^-$.

The proposed electronic structure difference between complexes **1** and **2** ($\{Fe^{+1}(^{\bullet}NO)_2\}^9$ versus $\{Fe^{-1}(NO^+)_2\}^9$ or combinations of $\{Fe^{+1}(^{\bullet}NO)_2\}^9$ and $\{Fe^{-1}(NO^+)_2\}^9$) is also reflected in the NO ligand lability of complexes **1** and **2**. The inertness of NO ligand of complex **1** was demonstrated by exposing the THF solution of $[Se_5Fe(^{15}NO)_2]^-$ to ^{14}NO atmosphere. Complex $[Se_5Fe(^{15}NO)_2]^-$ was stable under purge of ^{14}NO gas in THF at room temperature for half-an-hour. At the end of this time, the product was all $[Se_5Fe(^{15}NO)_2]^-$. In contrast to $[Se_5Fe(^{15}NO)_2]^-$, complex $[S_5Fe(^{15}NO)_2]^-$ did show the reversibility of NO ligand lability to yield $[S_5Fe(^{14}NO)_2]^-$ when a THF solution of $[S_5Fe(^{15}NO)_2]^-$ was exposed to ^{14}NO atmosphere.

3.4. Cell culture experiments

Complex **2′** is slightly soluble in H_2O but is soluble in H_2O–DMSO. The disappearance of IR ν_{NO} spectrum (ν_{NO}: 1706 m, 1743 s cm^{-1}) demonstrates the instability of complex **2′** dissolving in H_2O–DMSO solution at room temperature. In order to demonstrate complex **2′** serving as a NO-release reagent, the commercial NO sensor (WPI) was used to identify the NO released when complex **2′** was dissolved in an aerated pH 7.4 aqueous solution (H_2O–DMSO). The decay of the NO electrochemical signals can be attributed to NO autoxidation in this solution. On the basis of NO-analyzer experiments, light accelerates the release of NO when dissolving complex **2′** in aqueous solution (volume ratio of 1:500 for DMSO:PBS (pH 7.4)).

The Roussin's black/red salts have been used to deliver NO photochemically to greatly decrease the survival fractions of the cell cultures when exposed to γ-radiation [15,36]. Treatment of human erythroleukemia K562 cells with UV-A alone had little effect on the survival. This complex **2′** proved to be not cytotoxic or cytostatic to be used in such experiments, with percentage survival of 99% for treatment with 1 μM complex **2′** solution or 1 μM $[S_5Fe(\mu\text{-}S)_2FeS_5]^{2-}$ solution. However, treatment with 100 μM complex **2′** solution proved to be quite toxic; the cells were noticeably stained with trypan blue (viable cells exclude trypan blue, while dead cells stain blue due to membrane disruption) and the percentage of survival was less than 10%. Also investigated here are attempts to use complex **2′** as vehicle for delivering NO to cancer cell cultures to induce cell death. Fig. 5 shows the survival rate of human erythroleukemia K562 cell cultures when subjected to complex **2′** and complex **2′** combined with UV-A light in different cell numbers. Obviously, complex **2′** treated cancer cells exposed to UV-A light greatly decreased the percentage survivals of the cell cultures giving the respective percentage of survivals 39%, 26%, and 14%, respectively. This result implicates that complex **2′** may serve as a potentially photochemical reagent in pharmacological delivery of NO to various tumors.

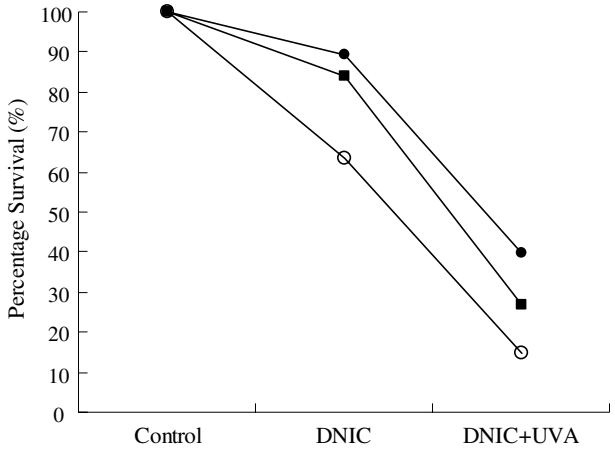

Fig. 5. Percentage survival of human erythroleukemia K562 cells in the presence of 10 μM DNICs **2′** with or without UV-A light for different cell numbers 2×10^5 (○), 3×10^5 (■), 4×10^5 (●).

3.5. X-ray crystal structure

Figs. 1 and 3 display the thermal ellipsoid plot of the anionic complexes **1** and **2′**, respectively. Crystallographic data, selected bond distances and bond angles are given in Tables 1 and 2, respectively. The nitrosyls are slightly bent (∠Fe–N(1)–O(1) = 170.1(6)° and ∠Fe–N(2)–O(2) = 167.4(7)°) and flared toward each other (∠O(1)–Fe–O(2) = 103.4° versus ∠N(1)–Fe–N(2) = 115.6°; attracto conformation). X-ray structure determination of complex **1** shows that the $FeSe_5$ ring in the chair conformation is similar to its analogue, $[S_5Fe(NO)_2]^-$ [22]. The Fe–Se average distance of 2.412(1) Å is shorter than those of complexes *fac*-$[Fe^{II}(CO)_3(SePh)_3]^-$ ($Fe–Se_{ave}$ = 2.459(2) Å) [37], and $[Se_5Fe(\mu\text{-}Se)_2FeSe_5]^{2-}$ ($Fe–Se_{ave}$ = 2.424(2) Å) [30], but comparable to the Fe–SePh distance (2.395(1) Å (average)) in $[(PhSe)_2Fe(NO)_2]^-$ [33]. Alternation in Se—Se bond lengths, spanning the range from 2.320(1) to 2.326(1) Å, is observed in complex **1**. The Fe–N(2)–O(2) bond is off linearity by 13° and differs from the Fe–N(1)–O(1) bond, which is coordinated in a nearly linear mode with Fe–N(1)–O(1) bond angle of 170.1(6)° in complex **1**.

Table 1
Crystallographic data for the complexes [PPN][$(Se)_5Fe(NO)_2$] (**1**) and [K-18-crown-6-ether][$S_5Fe(NO)_2$] (**2′**)

Complexes	**1**	**2′**
Formula	$C_{36}H_{30}FeN_3O_2P_2Se_5$	$C_{36}H_{72}Fe_3K_3N_6O_{24}S_{15}$
Formula weight	1049.22	1738.75
Crystal size	0.35 × 0.35 × 0.32	0.30 × 0.25 × 0.25
Crystal system	monoclinic	triclinic
Space group	$P2_1/c$	$P\bar{1}$
Unit cell dimensions		
a (Å)	11.2637(6)	9.5120(1)
b (Å)	11.7431(6)	14.2804(1)
c (Å)	29.1076(15)	27.2859(2)
α (°)	90.00	90.2025(5)
β (°)	94.255(1)	93.5272(4)
γ (°)	90.00	90.6861(5)
Volume (Å^3)	3839.5(3)	3699.06(5)
Z	4	2
D_{calc} (g cm^{-3})	1.815	1.561
F(000)	2036	1794
θ Range (°)	1.40–27.5	1.43–27.5
Total number of reflections	8823	67617
Number of unique data (R_{int})	6206	16986 (0.0434)
Number of parameters	467	838
R_1,[a] wR_2[b] (%) [$I > 2\sigma(I)$]	4.20, 9.73	5.30, 15.21
R_1,[a] wR_2[b] (%) all data	7.19, 11.51	7.87, 16.52
$\Delta\rho_{min}$ and $\Delta\rho_{max}$(e Å^{-3})	0.082 and −0.602	1.503 and −0.597

[a] $R = \sum||(F_o - F_c)|/\sum F_o$.
[b] $RwF^2 = \sum w(F_o^2 - F_c^2)^2/\sum[w/(F_o^2)^2]^{1/2}$.

Table 2
Selected bond distances and angles of complexes [PPN][$(Se)_5Fe(NO)_2$] (**1**) and [K-18-crown-6-ether][$S_5Fe(NO)_2$] (**2′**)

	1	**2′**
Fe–N_1 (Å)	1.680(4)	1.682(3)
Fe–N_2	1.670(4)	1.675(4)
Fe–Se_1/Fe–S_1	2.400(8)	2.2859(11)
Fe–Se_5/Fe–S_5	2.4103(8)	2.742(11)
N_1–O_1	1.166(4)	1.176(4)
N_2–O_2	1.174(5)	1.176(4)
Se–Se_{avg}/S–S_{avg}	2.3238(6)	2.0538(8)
∠N_1–Fe–N_2	116.62(18)	121.26(17)
N–Fe–Se_{avg}/N–Fe–S_{avg}	108.80(0)	107.87(1)
Fe–N–O_{avg}	107.0	171.8(8)
Se_1–Fe–Se_5/S_1–Fe–S_5	112.23(3)	107.60(4)

See Figs. 1 and 2.

4. Conclusion and comments

Complexes **1** and **2′** were synthesized by the reaction of $[Fe(CO)_3(NO)]^-$ with Se_8 and S_8 in THF solution. Facile conversion of complex **1** to **2** and **5**–**7** was observed by reacting complex **1** with one equivalent of S_8 and $(RS)_2$ in THF, respectively. This result shows that the $\{Fe(NO)_2\}^9$ core has more affinity to the thiolates as compared to selenolate ligand. Compared to complex **2**, magnetic susceptibility measurements (temperature-dependent, μ_{eff} = 1.77 BM (4 K) and μ_{eff} = 3.29 BM (300 K)), EPR spectroscopy (g = 2.064) and NO-trapping experiments support the fact that the dinitrosyl iron complex **1** might be assigned as a resonance hybrid of $\{Fe^{+1}(^{\bullet}NO)_2\}^9$ (minor) and $\{Fe^{-1}(NO^+)_2\}^9$ (major) [21,22]. On the basis of previous investigation and this study, the electronic structure of $\{Fe(NO)_2\}$ core of $\{Fe(NO)_2\}^9$ DNICs $[(L)_2Fe(NO)_2]^-$ (L = Se_5, S_5, thiolate) is best described as a dynamic resonance hybrid of $\{Fe^{+1}(^{\bullet}NO)_2\}^9$ and $\{Fe^{-1}(NO^+)_2\}^9$, modulated by the coordinated ligands. The variation of the p value from the magnetic susceptibility fit ($\chi_M^{exp} = (1-p)\chi_M(\{Fe^{+1}(^{\bullet}NO)_2\}^9) + p\chi_M(\{Fe^{-1}(^{+}NO)_2\}^9)$) is significantly controlled by the thiolate/selenolate ligands bound to the $\{Fe(NO)_2\}$ core, as shown in Scheme 2.

This study also shows that thiolates or selenolates bound to the $\{Fe(NO)_2\}^9$ core may serve to modulate the NO-release ability of DNICs. As has been known, characterization of both protein-bound and low-molecular weight DNICs (LMW-DNICs) in vitro has been made possible via their distinctive EPR signals at g = 2.03 [1–11]. In this study, the findings, EPR signal of g = 2.064 for complex **1** and the poor NO-release activity of **1** and $[(PhSe)_2Fe(NO)_2]^-$, imply that the LMW-DNICs and protein-bound DNICs may not exist with selenocysteine residues of proteins

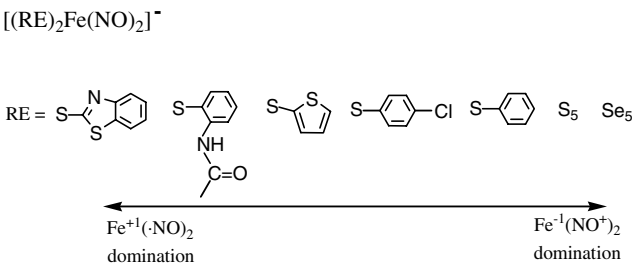

Scheme 2.

as ligands. That one equivalent of $[Fe(S,S\text{-}CN(Et)_2)_3]$ in the presence of one equivalent of S_8 was required to completely convert one equivalent of complex **2** into $[S_5Fe(\mu\text{-}S)_2FeS_5]^{2-}$ along with the formation of $[(NO)Fe(S,S\text{-}CN(Et)_2)_2]$ demonstrates that complexes **2**/**2′** act as a NO-delivering species. This study also shows that complex **2′** may serve as a potentially NO-delivering reagent in cell killing in human erythroleukemia K562 cell cultures [38–40].

Acknowledgment

We thank the National Science Council (Taiwan) for support of this work.

Appendix A. Supplementary data

Supplementary data associated with this article can be found, in the online version, at doi:10.1016/j.ica.2006.02.035.

References

[1] M.C. Kennedy, W.E. Antholine, H. Beinert, J. Biol. Chem. 272 (1997) 20340.
[2] R.H. Morse, S.I. Chan, J. Biol. Chem. 255 (1980) 7876.
[3] J.C. Drapier, C. Pellat, Y. Henry, J. Biol. Chem. 266 (1991) 10162.
[4] M. Lee, P. Arosio, A. Cozzi, N.D. Chasteen, Biochemistry 33 (1994) 3679.
[5] M. Lepoivre, J.-M. Flaman, P. Bobé, G. Lemaire, Y. Henry, J. Biol. Chem. 269 (1994) 21891.
[6] M.W. Foster, J.A Cowan, J. Am. Chem. Soc. 121 (1999) 4093.
[7] V.M. Sellers, M.K. Johnson, H.A. Dailey, Biochemistry 35 (1996) 2699.
[8] A.F. Vanin, Biochem (Moscow) 63 (1998) 782.
[9] P.C. Ford, J. Bourassa, K. Miranda, B. Lee, I. Lorkovic, S. Boggs, S. Kudo, L. Laverman, Coord. Chem. Rev. 171 (1998) 185.
[10] C.E. Cooper, Biochim. Biophys. Acta 1411 (1999) 290.
[11] J.L. Alencar, K. Chalupsky, M. Sarr, V. Schini-Kerth, A.F. Vanin, J.-C. Stoclet, B. Muller, Biochem. Pharmacol. 66 (2003) 2365.
[12] R.H. Holm, P. Kennepohl, E.I. Solomon, Chem. Rev. 96 (1996) 2239.
[13] T.C. Stadtman, Annu. Rev. Biochem. 65 (1996) 83.
[14] A. Böck, K. Forchhammer, J. Heider, W. Leinfelder, G. Sawers, B. Veprek, F. Zinoni, Mol. Microbiol. 5 (1991) 515.
[15] J. Bourassa, W. DeGraff, S. Kudo, D.A. Wink, J.B. Mitchell, P.C. Ford, J. Am. Chem. Soc. 119 (1997) 2853.
[16] A.R. Butler, C. Glidewell, M.-H. Li, Adv. Inorg. Chem. 32 (1988) 335.
[17] A.R. Butler, C. Glidewell, A.R. Hyde, J.C. Walton, Inorg. Chim. Acta 106 (1985) L7.
[18] A.R. Butler, C. Glidewell, A.R. Hyde, J.C. Walton, Polyhedron 4 (1985) 797.
[19] W. Beck, R. Grenz, F. Götzfried, E. Vilsmaier, Chem. Ber. 114 (1981) 3184.
[20] A.R. Butler, I.L. Megson, Chem. Rev. 102 (2002) 1155.
[21] M.-L. Tsai, C.-C. Chen, I.-J. Hsu, S.-C. Ke, C.-H. Hsieh, K.-A. Chiang, G.-H. Lee, Y. Wang, J.-M. Chen, J.-F. Lee, W.-F. Liaw, Inorg. Chem. 43 (2004) 5159.
[22] F.-T. Tsai, S.-J. Chiou, M.-C. Tsai, M.-L. Tsai, H.-W. Huang, M.-H. Chiang, W.-F. Liaw, Inorg. Chem. 44 (2005) 5872.
[23] H. Ding, B. Demple, Proc. Natl. Acad. Sci. USA 97 (2000) 5146.
[24] L. Hedberg, K. Hedberg, S.K. Satija, B.I. Swanson, Inorg. Chem. 24 (1985) 2766.
[25] T.W. Hayton, P. Legzdins, W.B. Sharp, Chem. Rev. 102 (2002) 935.
[26] C.T.-W. Chu, L.F. Dahl, Inorg. Chem. 16 (1977) 3245.
[27] M.J. Scott, R.H. Holm, Angew. Chem. Int. Ed. Engl. 32 (1993) 564.
[28] S. Fujii, K. Kobayashi, S. Tagawa, Y. Tetsuhiko, J. Chem. Soc., Dalton Trans. (2000) 3310.
[29] D. Coucouvanis, D. Swenson, P. Stremple, N.C. Baenziger, J. Am. Chem. Soc. 101 (1979) 3392.
[30] H. Strasdeit, B. Krebs, G. Henkel, Inorg. Chim. Acta 89 (1984) L11.
[31] R.H. Blessing, Acta Crystallogr., Sect. A 51 (1995) 33.
[32] G.M. Sheldrick, SHELXTL, Program for Crystal Structure Determination, Siemens Analytical X-ray Instruments Inc., Madison, WI, 1994.
[33] W.-F. Liaw, C.-Y. Chiang, G.-H. Lee, S.-M. Peng, C.-H. Lai, M.Y. Darensbourg, Inorg. Chem. 39 (2000) 480.
[34] H. Strasdeit, B. Krebs, G.Z. Henkel, Naturforsch. 41B (1986) 1357.
[35] J.H. Enemark, R.D. Feltham, Coord. Chem. Rev. 13 (1974) 339.
[36] J.B. Mitchell, D.A. Wink, W. DeGraff, J. Gamson, L.K. Keefer, M.C. Krishna, Cancer Res. 53 (1993) 5845.
[37] W.-F. Liaw, C.-H. Lai, C.-K. Lee, G.-H. Lee, S.-M. Peng, J. Chem. Soc., Dalton Trans. (1993) 2421.
[38] P.C. Ford, S. Wecksler, Coord. Chem. Rev. 249 (2005) 1382, and references therein.
[39] P.C. Ford, J. Bourassa, B. Lee, I. Lorkovic, K. Miranda, L. Laverman, Chem. Rev. 171 (1998) 185, and references therein.
[40] P.C. Ford, J. Bourassa, Coord. Chem. Rev. 200–202 (2000) 887, and references therein.